Extraction of the Muon Beam Frequency Distribution via the Fourier Analysis of the Fast Rotation Signal

Daniel Seleznev[1], Antoine Chapelain[1], and David Rubin[1]

[1]Department of Physics, Cornell University, Ithaca, NY 14850

November 13, 2017

Contents

1 Introduction **2**

2 Fast Rotation **2**
2.1 What is Fast Rotation? . . . 2
2.2 Analytical Description . . . 3
2.3 Fast Rotation Signal Examples . . . 3
2.3.1 Gaussian Momentum Offset Distribution and No Longitudinal Spread . . . 3
2.3.2 Gaussian Momentum Offset Distribution and Gaussian Longitudinal Spread . . . 4

3 Fourier Analysis of the Fast Rotation Signal **5**
3.1 Mathematical Background . . . 5
3.2 The Case of Initially Zero Bunch Length . . . 6
3.3 Symmetric Bunch Length Distribution $\xi(t)$ . . . 7
3.4 Asymmetric Longitudinal Bunch Distribution . . . 9
3.5 Physical Interpretation of the Fourier Transform of the Fast Rotation Signal . . . 11
3.6 Taking the Fourier integral at a Finite Upper Bound . . . 11
3.7 Corrections to the Fourier Transform . . . 12
3.8 Fourier Analysis Examples . . . 14
3.8.1 Analysis for a Gaussian Energy Offset Distribution with Initially Zero Bunch Length . 14
3.8.2 Analysis for a Gaussian Energy Offset Distribution and Gaussian Longitudinal Distribution . . . 15

4 Appendix **16**
4.1 Corrections to the Fourier Transform . . . 16
4.1.1 First Consideration . . . 16
4.1.2 Second Consideration . . . 17

1 Introduction

The Fermilab E989 Muon g-2 experiment aims to measure the anomalous magnetic moment of the muon a_μ to a precision of 0.14 ppm. The experiment relies on the storage of muons inside a weak focusing ring, with a continuous C-shape dipole magnet occupying its entirety (44.7 m circumference). The dipole generates a vertical and highly homogenous 1.45 T magnetic field to provide radial focusing for muon storage. The field intensity corresponds to storing muons with a design momentum of 3.094 GeV/c onto the design orbit (7.112 m radius), on which the muons undergo a cyclotron motion with a revolution frequency of 149.1 ns. Vertical focusing is provided by four electrostatic quadrupoles (ESQs) located around the ring.

The final extraction of a_μ is performed via the measurement of the intensity of the magnetic field in terms of the Larmor precession frequency of a free proton

$$\hbar\omega_p = 2\mu_p|\vec{B}| \tag{1}$$

and the precession frequency ω_a of the muon's spin about its momentum. ω_a is obtained by subtracting the cyclotron frequency ω_C from the total spin precession frequency of the muon ω_S:

$$\omega_a = \omega_S - \omega_C \tag{2}$$

In the presence of the electric field, the vectorial form of ω_a is

$$\vec{\omega}_a = -\frac{Q}{m}\left[a_\mu\vec{B} - \left(a_\mu - \frac{1}{\gamma^2-1}\right)\frac{\vec{\beta}\times\vec{E}}{c}\right] \tag{3}$$

The term proportional to $\vec{\beta}\times\vec{E}$ in Eq. (3) corresponds to the electric field contribution to ω_a. One can see that if γ is chosen such that $(\gamma^2-1)^{-1} = a_\mu$, the contribution disappears. If muons are launched at the magic momentum of 3.094 GeV/c, this value of γ is achieved and the electric field contribution vanishes in first order. However, there exists a second order contribution arising from the fact that the stored muon beam has a momentum spread of about 0.1%. This effect is non-negligible and needs to be taken care of. The correction to ω_a due to the electric field was estimated by E821 to be 0.47 ± 0.05 ppm for the 2001 data set for the low n-value data set. The final E821 result for a_μ has a 0.54 ppm precision, which is of the order of the electric field correction. The correction for the electric field contribution to ω_a is obtained from the muon revolution frequency distribution which is the result of a modified Fourier analysis of the so-called fast rotation signal (FRS). The technique was created for E821, but we independently re-derive its following key aspects: the analysis for when the beam features a longitudinal spread, and the analysis if beam detection occurs at late times.

2 Fast Rotation

2.1 What is Fast Rotation?

Fast rotation refers to the cyclotron motion in the ring, which has a revolution frequency of 6.706 MHz (period of 149.1 ns) for muons propagating on the design orbit with the design momentum. The fast rotation signal corresponds to the evolution of the beam as it propagates around the ring. The momentum spread of the beam makes it decohere (or debunch). To understand how the momentum spread leads to decoherence, one has to remember that the orbit radius for a fixed magnetic field is set by the momentum of the particle. Particles injected on the design orbit but with different momenta will have different radii R. Since the muons are highly relativistic, their speeds are nearly independent of their momenta ($dv/dp \approx 0$). The period of revolution of each muon is given by $T = 2\pi R/v = 2\pi p/(qvB)$, where $p = qBR$, so higher momenta muons will complete a revolution slower and have larger orbital radii than lower momenta muons, leading to a distribution of revolution frequencies. So a beam will evolve from having from having a limited longitudinal extension to filling the entirety of the ring.

2.2 Analytical Description

Imagine that the initial muon distribution has zero emittance (no transverse size), zero momentum spread and zero bunch length (no longitudinal extension). The particles share a common revolution period T and the time dependence of the intensity signal at a fixed point (signal measured at a fiber harp for example) is

$$I(t) = \sum_{n=0}^{\infty} \delta\left(t - \left(n + \frac{\theta}{2\pi}\right) T\right)$$

where n corresponds to the number of completed muon revolutions in the ring relative to the point, and θ is the azimuthal position of the point in the ring. A particle with energy offset Δ will have a momentum of $p(1+\Delta)$. Since the period of revolution is directly proportional to p in the relativistic regime, the particle will thus have a period of $T(1+\Delta)$, so that

$$I(t, \Delta) = \sum_{n=0}^{\infty} \delta\left(t - \left(n + \frac{\theta}{2\pi}\right) T\,(1+\Delta)\right)$$

A particle with a temporal offset t' as well as an energy offset Δ will generate an intensity signal given by [1]

$$I(t, \Delta, t') = \sum_{n=0}^{\infty} \delta\left(t - t' - \left(n + \frac{\theta}{2\pi}\right) T\,(1+\Delta)\right) \tag{4}$$

If there is a distribution of momentum offsets $\rho(\Delta)$ and a distribution of initial temporal offsets $\xi(t)$, the fast rotation signal at the point is then given by

$$S(t) = \sum_{n=0}^{\infty} \int \xi(t')dt' \int \rho(\Delta)\delta\left(t - t' - nT\,(1+\Delta)\right) d\Delta$$

Integrating, we get that

$$S(t) = \sum_{n=0}^{\infty} \int \xi(t')dt' \int \rho(\Delta) \frac{\delta\left(\Delta - \left(\frac{t-t'}{nT} - 1\right)\right)}{nT} d\Delta =$$

$$\sum_{n=0}^{\infty} \int \xi(t') \frac{\rho\left(\frac{t-t'}{nT} - 1\right)}{nT} dt' \tag{5}$$

2.3 Fast Rotation Signal Examples

2.3.1 Gaussian Momentum Offset Distribution and No Longitudinal Spread

If $\xi(t) = \delta(t)$, formula (5) reduces to

$$S(t) = \sum_{n=0}^{\infty} \frac{\rho\left(\frac{t}{nT} - 1\right)}{nT} \tag{6}$$

Let

$$\rho(\Delta) = \begin{cases} \frac{e^{-\Delta^2/2\Delta_0^2}}{\sqrt{2\pi}\Delta_0}, \text{ if } \Delta \in [-\Delta_c, \Delta_c] \\ 0, \text{ if } \Delta \notin [-\Delta_c, \Delta_c] \end{cases} \tag{7}$$

where $\Delta_c = 0.25\%$ is the cutoff offset corresponding to the presence of the vacuum chambers for the g-2 storage ring. We see an example of such an FRS in Figure 1.

[1] The expression $(n + \theta/2\pi)T$ will be denoted thereafter nT for improved text clarity, unless otherwise noted

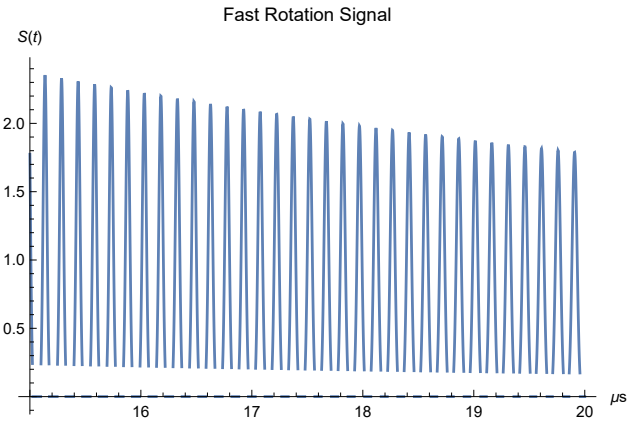

Figure 1: FRS for a beam with a cutoff Gaussian momentum distribution with a spread of 0.112% and no longitudinal spread or transverse emittance, as seen by a detector at a point halfway around the storage ring. The beam is observed to debunch with the increasing width of consecutive peaks.

2.3.2 Gaussian Momentum Offset Distribution and Gaussian Longitudinal Spread

If

$$\xi(t) = \frac{e^{-t^2/(2\sigma_t^2)}}{\sqrt{2\pi}\sigma_t}$$

and $\rho(\Delta)$ is the same as earlier, then we have that

$$S(t) = \int_{-\infty}^{\infty} \frac{e^{-t'^2/(2\sigma_t^2)}}{\sqrt{2\pi}\sigma_t} \left(\sum_{n=0}^{\infty} \frac{\rho\left(\frac{t-t'}{nT} - 1\right)}{nT} \right) dt' = \sum_{n=0}^{\infty} \frac{1}{\sqrt{2\pi}\sigma_t nT} \int_{-\infty}^{\infty} e^{-t'^2/(2\sigma_t^2)} \rho\left(\frac{t-t'}{nT} - 1\right) dt'$$

The argument of ρ in the integral above doesn't vanish if

$$-\Delta_c \leq \frac{t-t'}{nT} - 1 \leq \Delta_c \Rightarrow t - (1+\Delta_c)nT \leq t' \leq t - (1-\Delta_c)nT$$

so the integral may be rewritten as

$$\sum_{n=0}^{\infty} \frac{1}{\sqrt{2\pi}\sigma_t nT} \int_{t-(1+\Delta_c)nT}^{t-(1-\Delta_c)nT} e^{-t'^2/(2\sigma_t^2)} \rho\left(\frac{t-t'}{nT} - 1\right) dt' =$$

$$\sum_{n=0}^{\infty} \frac{e^{-(t-nT)^2/2\Delta_0'^2} \left(\mathrm{Erf}\left[\frac{\Delta_c \sigma_t^2 + \Delta_0^2 nT(t-(1-\Delta_c)nT)}{\sqrt{2}\Delta_0 \sigma_t \Delta_0'} \right] - \mathrm{Erf}\left[\frac{-\Delta_c \sigma_t^2 + \Delta_0^2 nT(t-(1+\Delta_c)nT)}{\sqrt{2}\Delta_0 \sigma_t \Delta_0'} \right] \right)}{2\sqrt{2\pi}\Delta_0'} \tag{8}$$

where

$$\Delta_0' = \sqrt{\sigma_t^2 + \Delta_0^2 n^2 T^2}$$

An example of such a FRS is given in Figure 2.

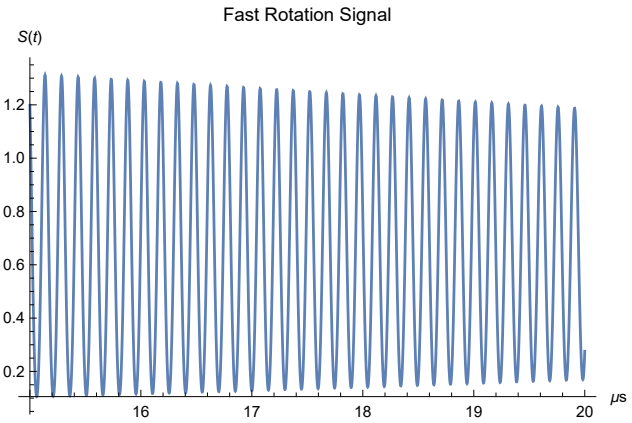

Figure 2: FRS for a beam with a cutoff Gaussian momentum distribution of spread 0.112% and with a Gaussian longitudinal distribution with $\sigma_t = 25$ ns, as seen by a detector at a point halfway around the storage ring.

3 Fourier Analysis of the Fast Rotation Signal

3.1 Mathematical Background

Definition 1 (Fourier's transform and inverse transform) *Given a function f, its Fourier transform is*

$$\hat{f}(x) = \frac{1}{\sqrt{2\pi}} \int_{-\infty}^{\infty} f(t) e^{ixt} dt$$

and its inverse Fourier transform is

$$\tilde{f}(x) = \frac{1}{\sqrt{2\pi}} \int_{-\infty}^{\infty} f(t) e^{-ixt} dt$$

If f is absolutely integrable, then the Fourier transforms of f always exist. It is easy to check that $f = \tilde{\hat{f}} = \hat{\tilde{f}}$.

Theorem 1 (Fourier's Integral) *For any piecewise continuous, piecewise differentiable, and absolutely integrable function f, the following equality holds:*

$$f(x) = \frac{1}{\pi} \int_0^{\infty} d\omega \int_{-\infty}^{\infty} f(t) \cos \omega(t - x) dt$$

If f is even, then Fourier's integral simplifies to

$$f(x) = \frac{2}{\pi} \int_0^{\infty} \cos \omega x d\omega \int_0^{\infty} f(t) \cos \omega t dt$$

Suppose f is a piecewise continuous, piecewise differentiable, and absolutely integrable function on $[0, \infty)$. If we extend f to an even function defined on the whole real line, then the formula above is valid for the extension. In particular, it is also valid for $x \geq 0$.

Theorem 2 (Convolution Theorem) *The convolution of two functions f and g is defined to be*

$$(f * g)(t) = \frac{1}{\sqrt{2\pi}} \int_{-\infty}^{\infty} f(\tau) g(t - \tau) d\tau$$

The convolution theorem states that

$$\widehat{f * g} = \hat{f}\hat{g} \text{ and } \widetilde{f * g} = \tilde{f}\tilde{g}$$

3.2 The Case of Initially Zero Bunch Length

If $\xi(t) = \delta(t)$, the FRS of the beam at a detector with azimuthal position θ is given by

$$S(t) = \sum_{n=0}^{\infty} \frac{\rho\left(\frac{t}{(n+\theta/2\pi)T} - 1\right)}{(n + \theta/2\pi)T}$$

where n is the turn number and T the cyclotron period of a particle on the design orbit. The muon beam is expected to have a narrow spread in revolution frequencies, $(\omega - \omega_0)/\omega \sim 10^{-3}$ where ω_0 is the design orbit frequency, due to the aperture size of the storage region. As a result the beam will spread negligibly in the longitudinal direction during the first turn. We thus have that

$$\frac{\theta}{2\pi} = \frac{t_0}{T}$$

where t_0 is the time the center of mass of the longitudinal distribution first passes the detector. We may thus rewrite the FRS above as

$$S(t) = \sum_{n=0}^{\infty} \frac{\rho\left(\frac{t}{nT+t_0} - 1\right)}{nT + t_0}$$

We next assume that $\rho(\Delta)$ is sufficiently well behaved so as to be absolutely integrable, piecewise continuous and piecewise differentiable. Define $\mathcal{S}(t) \equiv S(t + t_0)$. Extend $\mathcal{S}$ to the entire real line as an even function. The extension is justified by the fact that $S(t)$ is time-reversal symmetric about t_0. By Theorem 1, we may express $\mathcal{S}$ as

$$\mathcal{S}(t) = \frac{2}{\pi} \int_0^{\infty} \cos\omega t d\omega \int_0^{\infty} \mathcal{S}(t') \cos\omega t' dt'$$

We then recover $S(t)$:

$$S(t + t_0) = \frac{2}{\pi} \int_0^{\infty} \cos\omega t d\omega \int_0^{\infty} S(t' + t_0) \cos\omega t' dt' =$$

$$\frac{2}{\pi} \int_0^{\infty} \cos\omega t d\omega \int_{t_0}^{\infty} S(t') \cos\omega(t' - t_0) dt' \Rightarrow$$

$$S(t) = \frac{2}{\pi} \int_0^{\infty} \cos\omega(t - t_0) d\omega \int_{t_0}^{\infty} S(t') \cos\omega(t' - t_0) dt'$$

But we also know from Definition 1 that

$$\mathcal{S}(t) = \tilde{\hat{\mathcal{S}}}(t) = \frac{1}{2\pi} \int_{-\infty}^{\infty} e^{-i\omega t} d\omega \int_{-\infty}^{\infty} \mathcal{S}(t') e^{i\omega t'} dt' =$$

$$\frac{1}{2\pi} \int_{-\infty}^{\infty} e^{-i\omega t} d\omega \int_{-\infty}^{\infty} \mathcal{S}(t')(\cos\omega t' + i \sin\omega t') dt' = \frac{1}{2\pi} \int_{-\infty}^{\infty} e^{-i\omega t} d\omega \int_{-\infty}^{\infty} \mathcal{S}(t') \cos\omega t' dt' =$$

$$\frac{1}{\sqrt{2\pi}} \int_{-\infty}^{\infty} \hat{\mathcal{S}}(\omega) e^{-i\omega t} d\omega$$

where we used the fact that $\mathcal{S}$ is an even function, and the integral of the product of an even and odd function vanishes. From the preceding expression we now see that $\hat{\mathcal{S}}$ is an even function. So we write

$$\frac{1}{\sqrt{2\pi}} \int_{-\infty}^{\infty} \hat{\mathcal{S}}(\omega) \cos\omega t d\omega = \sqrt{\frac{2}{\pi}} \int_0^{\infty} \hat{\mathcal{S}}(\omega) \cos\omega t d\omega = \frac{2}{\pi} \int_0^{\infty} \cos\omega t d\omega \int_0^{\infty} \mathcal{S}(t') \cos\omega t' dt'$$

We see that Fourier's integral is equivalent to applying the Fourier transform and inverse transform in succession. Hence

$$\hat{S}(\omega) = \sqrt{\frac{2}{\pi}} \int_{t_0}^{\infty} S(t) \cos \omega (t - t_0) dt \tag{9}$$

is the Fourier transform of S. So if we're given $\hat{S}(\omega)$, we may express S as

$$S(t) = \sqrt{\frac{2}{\pi}} \int_{0}^{\infty} \hat{S}(\omega) \cos \omega (t - t_0) d\omega = \frac{1}{\sqrt{2\pi}} \int_{-\infty}^{\infty} \hat{S}(\omega) \cos \omega (t - t_0) d\omega \tag{10}$$

Figure 3 features a comparison of the first harmonic of $\hat{S}_0(\omega)$ to the actual revolution frequency distribution of the muons for the FRS of Figure 1 and we see that they match. The actual distribution relates to $\rho(\Delta)$ in the following way. Given an offset Δ, the revolution frequency of a muon with that offset will be $f = \frac{f_0}{1+\Delta}$ where f_0 is the design frequency. Inverting the expression yields $\Delta = \frac{f_0 - f}{f}$. Therefore the frequency distribution is given by $\rho\left(\frac{f_0 - f}{f}\right)$. If $\rho(\Delta)$ is given by (7), then the frequency distribution is

$$\rho\left(\frac{f_0 - f}{f}\right) = \frac{e^{-(f_0 - f)^2 / 2 f^2 \Delta_0^2}}{\sqrt{2\pi}\Delta_0} \approx \frac{e^{-(f - f_0)^2 / 2\Delta_0^2 / T_0^2}}{\sqrt{2\pi}\Delta_0}$$

up to a normalization constant. The reason the approximation is made is because the frequency distribution is very narrow, $(f - f_0)/f \sim 10^{-3}$.

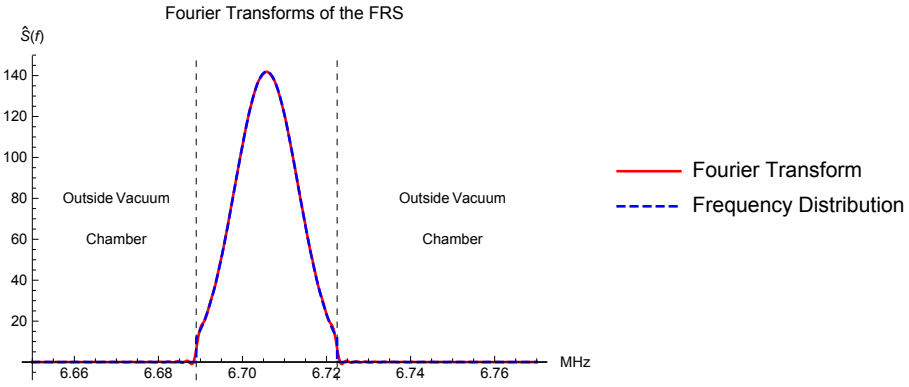

Figure 3: Comparison of the first harmonic of the Fourier transform of the FRS from Figure 1 to the actual muon revolution frequency distribution

3.3 Symmetric Bunch Length Distribution $\xi(t)$

Assuming that there is no initial correlation between muon revolution frequencies and longitudinal phases, there will exist a longitudinal offset distribution $\xi(t')$ which can be taken into account in a straightforward manner when performing the Fourier analysis. We call the fast rotation signal with no initial bunch length $S_0(t)$. The fast rotation signal is then

$$S(t) = \int \xi(t') S_0(t - t') dt' = \sqrt{2\pi} (\xi * S_0)(t)$$

as we saw earlier in the examples of fast rotation signals above. Ideally, the application of the convolution theorem would yield

$$\hat{S}(\omega) = \sqrt{2\pi} \hat{\xi}(\omega) \hat{S}_0(\omega) \tag{11}$$

However, we'll have neither $S_0(t)$ to work with directly, nor $\xi(t)$. We need to use $S(t)$ to get $\hat{S}(\omega)$.

We express $S_0(t - t')$ through Fourier's integral:

$$S_0(t - t') = \frac{2}{\pi} \int_{0}^{\infty} \cos \omega (t - t_0 - t') d\omega \int_{t_0}^{\infty} S_0(\bar{t}) \cos \omega (\bar{t} - t_0) d\bar{t} =$$

$$\sqrt{\frac{2}{\pi}}\int_0^\infty \hat{S}_0(\omega)\cos\omega(t-t_0-t')d\omega$$

Substituting this expression into the convolution integral, we get

$$S(t)=\sqrt{2\pi}(\xi * S_0)(t)=\int_{-\infty}^{\infty}\xi(t)S_0(t-t')dt'=\sqrt{\frac{2}{\pi}}\int_0^\infty \hat{S}_0(\omega)d\omega\int_{-\infty}^{\infty}\xi(t')\cos\omega(t-t_0-t')dt'$$

We let $\langle f(t)\rangle=\int f(t)\xi(t)dt$, so the expression above simplifies to

$$\sqrt{\frac{2}{\pi}}\int_0^\infty \hat{S}_0(\omega)\langle\cos\omega(t-t_0-t')\rangle d\omega=$$

$$\sqrt{\frac{2}{\pi}}\int_0^\infty \hat{S}_0(\omega)\langle\cos\omega(t-t_0)\cos\omega t'+\sin\omega(t-t_0)\sin\omega t'\rangle d\omega=$$

$$\sqrt{\frac{2}{\pi}}\left(\int_0^\infty \hat{S}_0(\omega)\langle\cos\omega t'\rangle\cos\omega(t-t_0)d\omega+\int_0^\infty \hat{S}_0(\omega)\langle\sin\omega t'\rangle\sin\omega(t-t_0)d\omega\right)$$

If $\xi(t')$ is even, $\langle\sin\omega t'\rangle=0$. We are then left with

$$S(t)=\sqrt{\frac{2}{\pi}}\int_0^\infty \hat{S}_0(\omega)\langle\cos\omega t'\rangle\cos\omega(t-t_0)d\omega \tag{12}$$

suggesting that $\hat{S}(\omega)=\hat{S}_0(\omega)\langle\cos\omega t'\rangle$. We can see that this is true by looking back at (11):

$$\hat{\xi}(\omega)=\frac{1}{\sqrt{2\pi}}\int_{-\infty}^{\infty}\xi(t')e^{i\omega t'}dt'=\frac{1}{\sqrt{2\pi}}\int_{-\infty}^{\infty}\xi(t')\cos\omega t'dt'=\frac{\langle\cos\omega t'\rangle}{\sqrt{2\pi}}$$

and therefore

$$\hat{S}(\omega)=\sqrt{2\pi}\hat{\xi}(\omega)\hat{S}_0(\omega)=\hat{S}_0(\omega)\langle\cos\omega t'\rangle \tag{13}$$

Thus (12) is the inverse Fourier transform, implying that

$$\hat{S}(\omega)=\sqrt{\frac{2}{\pi}}\int_{t_0}^{\infty}S(t)\cos\omega(t-t_0)dt \tag{14}$$

In Figure 4 we see the first harmonics of the Fourier transforms of an FRS with longitudinal spread from Formulas (11) and (14) compared to the actual frequency distribution. The momentum spread was a full Gaussian with a narrow spread of 0.05% and Gaussian longitudinal spread with $\sigma_t = 10$ ns. The momentum distribution was selected to be especially narrow so as to well approximate having most muons in the vacuum chamber with a negligible amount outside it, in order to simplify calculations. We see that the spectra and distribution match.

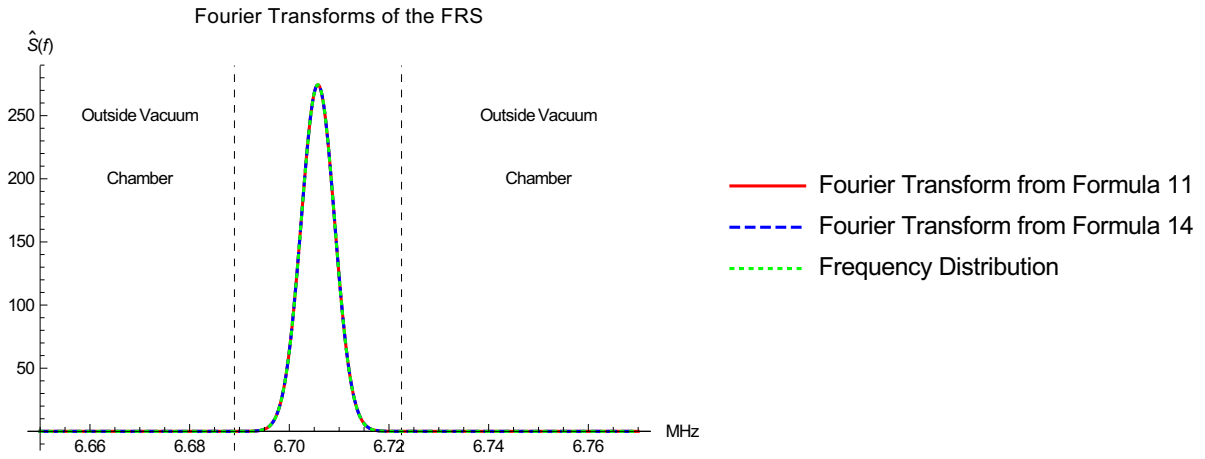

Figure 4: Comparison of the first harmonics of the Fourier transforms to the frequency distribution for an FRS with Gaussian momentum distribution of spread 0.05% and a Gaussian longitudinal spread with $\sigma_t = 10$ ns, as seen by a detector at a point halfway around the storage ring. $t_0 = 74.563$ ns.

3.4 Asymmetric Longitudinal Bunch Distribution

If $\xi(t')$ is not symmetric, then we are faced with the problem that $\hat{S}(\omega)$ features an imaginary component. Directly applying the convolution theorem yields

$$\hat{S}(\omega) = \hat{S}_0(\omega)\langle\cos\omega t'\rangle + i\hat{S}_0(\omega)\langle\sin\omega t'\rangle$$

which gives in the end an imaginary radial electric field correction.

To motivate a solution to this problem, we examine a specific example of an asymmetric longitudinal distribution. Suppose ξ is even about some point $\mu \neq 0$ (also the center of mass of the distribution), that is $\xi(x+\mu) = \xi(\mu - x)$. Let t_0 be the time that the center of mass of the beam first arrives at a given detector if μ were to equal 0. Then the actual arrival time of the center of mass of the bunch at the detector is $t_0' = t_0 + \mu$. The way that the beam appears to have evolved is the same as if it had a symmetric bunch profile and a detector at azimuthal position $\theta = 2\pi t_0'/T$ was used (see Figure 5). Define $\xi'(t) = \xi(t+\mu)$ and $S_0'(t) = S_0(t-\mu)$. Then the physical situation described by the triple (S_0', ξ', t_0') is the same as that described by (S_0, ξ, t_0). In fact we may see that they yield the same FRS $S(t)$:

$$\sqrt{2\pi}\xi'(t) * S_0'(t) = \int_{-\infty}^{\infty} \xi'(\tau)S_0'(t-\tau)d\tau = \int_{-\infty}^{\infty} \xi(\tau+\mu)S_0(t-\tau-\mu)d\tau = \int_{-\infty}^{\infty} \xi(\tau')S_0(t-\tau')d\tau' =$$

$$\sqrt{2\pi}\xi(t) * S_0(t) = S(t)$$

where we used the change of variables $\tau' = \tau + \mu$. But if we use (S_0', ξ', t_0') for the Fourier analysis, the imaginary term in $\hat{S}(\omega)$ vanishes, since we're now dealing with a familiar situation: a symmetric longitudinal distribution. Therefore

$$\hat{S}(\omega) = \sqrt{\frac{2}{\pi}} \int_{t_0'}^{\infty} S(t)\cos\omega(t - t_0')dt$$

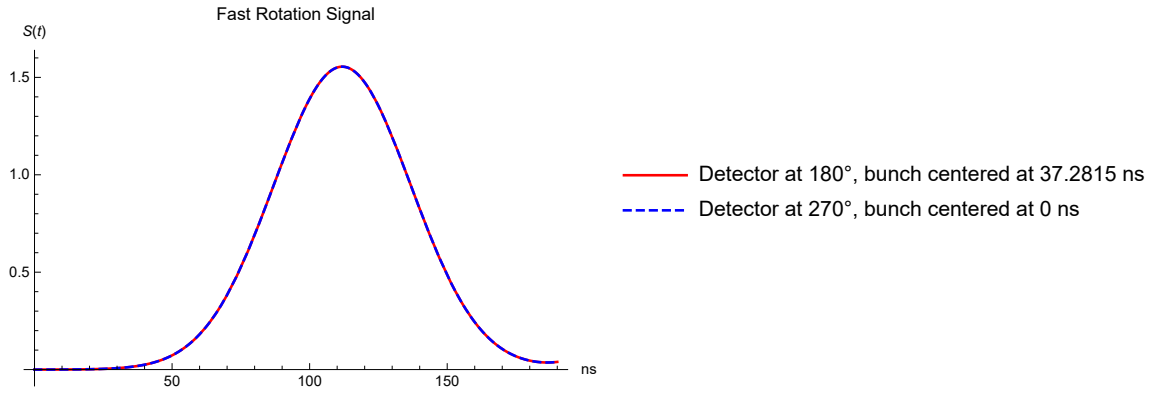

Figure 5: Both beams have Gaussian momentum distribution with a spread of 0.112% and Gaussian longitudinal spread with $\sigma_t = 25$ ns. The detector halfway around the ring is witnessing a beam with an offset Gaussian bunch, while the second is detecting one centered at the origin.

When $\xi(t)$ is an arbitrary asymmetric distribution, there is generally no unique symmetry point which makes it obvious how to redefine t_0. It may very well be that it is impossible for all frequencies to appear in the real component of the Fourier transform simultaneously. However, we are only concerned with extracting the first harmonic of the Fourier transform, so we may attempt to redefine t_0 in such a manner so as to have the first harmonic lie entirely in the real component of the Fourier transform.

To accomplish this, define a function

$$f(x) = \int_{\xi_- - x}^{\xi_+ - x} \xi(t+x) \sin \omega t dt \approx \int_{\xi_- - x}^{\xi_+ - x} \xi(t+x) \sin \omega_0 t dt$$

The approximation is made because we are concerned with extracting the first harmonic of the Fourier transform, where the frequency distribution is narrow and centered around ω_0. (ξ_-, ξ_+) is the domain of $\xi(t)$, and a point μ such that $f(\mu) = 0$ is then found. This effectively amounts to finding a new origin about which $\langle \sin \omega_0 t' \rangle = 0$, so that there is no imaginary component to the frequency distribution computed from the Fourier transform. In Figures 6 and 7 we see an example of a FRS with asymmetric bunch profile and the first harmonic of its Fourier transform compared to the actual revolution frequency distribution.

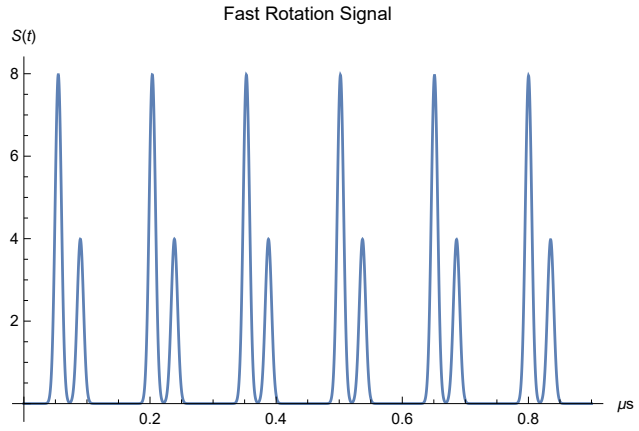

Figure 6: FRS for a beam with asymmetric longitudinal bunch profile seen by a detector halfway around the ring.

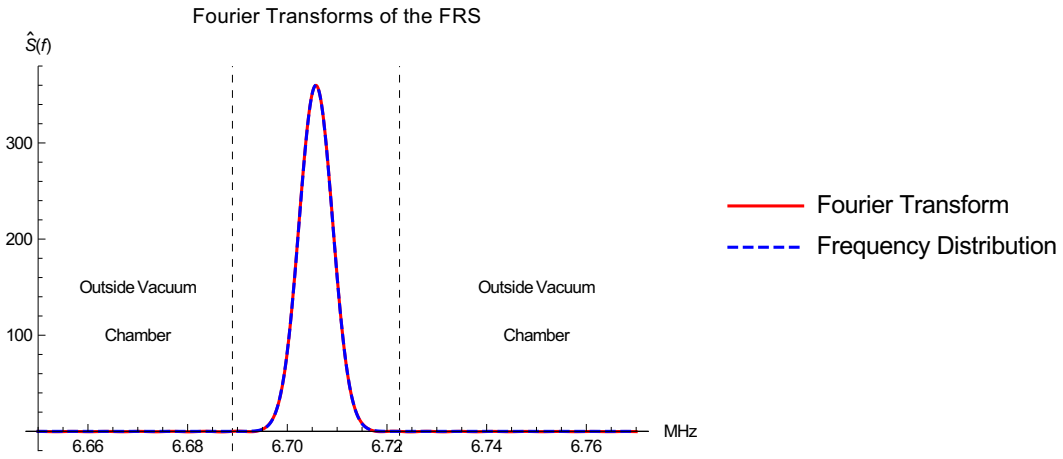

Figure 7: Comparison of the first harmonic of the Fourier transform of the FRS from Figure 6 to the actual muon revolution frequency distribution. The Fourier analysis used $t_0 = 65.086$ ns.

3.5 Physical Interpretation of the Fourier Transform of the Fast Rotation Signal

It makes sense to extract the frequency distribution of the muons from the FRS because the signal arises from the periodic detector hits of the muons. The periods of these hits depend on the revolution frequencies that the muons have, so the Fourier transform of the FRS reflects the relative amounts of these frequencies among the muons. The Fourier transform will [illegible]re peaks centered at integer multiples of the design frequency ω_0. However, the muons are restricted to the vacuum chamber due to the aperture size limiting the momentum spread. Therefore no frequencies may appear outside the aperture region.

3.6 Taking the Fourier integral at a Finite Upper Bound

As $t \to \infty$, the beam fully decoheres and the signal levels off at the average muon current $\langle I \rangle = eN_\mu/T$. Several turns after injection but before $t = +\infty$, the fast rotation signal appears to additionally oscillate at a single frequency close to the magic frequency. Since the fast rotation signal is expressed as sum of cosines, as t starts to get large each of the [illegible]nes begins to oscillate more rapidly, yielding cancellations, so only frequencies near the magic frequency contribute to the signal.

In the preceding Fourier integrals, the upper bound was $t = +\infty$, but in reality we must instead use an acceptable large time t_m. t_m must be a time at which $S(t)$ is exhibiting the asymptotic behavior just described. In that case we get a close approximation to the frequency spectrum, since the frequency content of $S(t)$ does not change much after t_m (the signal keeps oscillating at the same frequency after t_m, or does not oscillate at all and remains constant).

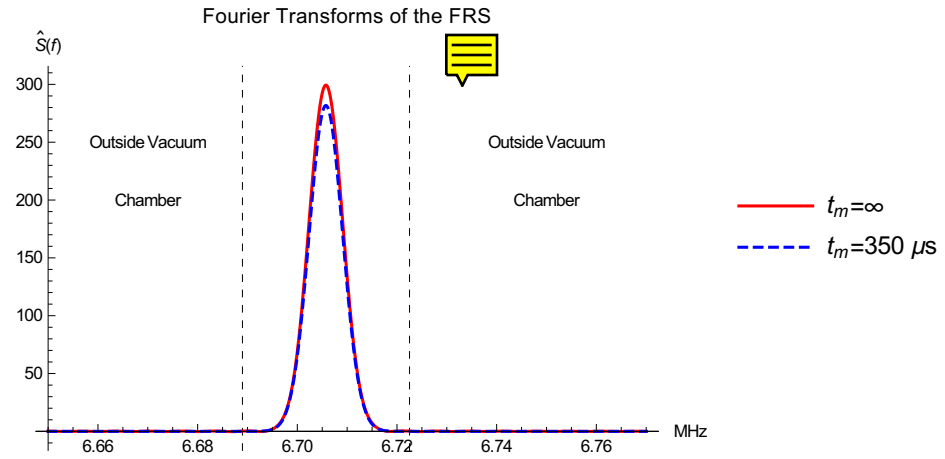

Figure 8: Comparison of spectra obtained using $t_m = 350\mu$s and ∞. Using $t_m = 350\mu$s yields a Gaussian distribution with spread identical to that of the actual distribution, but with amplitude off by factor

3.7 Corrections to the Fourier Transform

If the detector detects the muons at a time $t_s > t_0$, a fast rotation signal $S_1(t)$ which vanishes on (t_0, t_s) and equals the full fast rotation signal $S(t)$ on $[t_s, \infty)$ is observed. Taking the Fourier transform of $S_1(t)$, results in the frequency spectrum

$$\hat{S}_1(\omega) = \sqrt{\frac{2}{\pi}} \int_{t_s}^{\infty} S_1(t) \omega(t - t_0) dt \tag{15}$$

This is not the complete frequency spectrum as the following component is missing:

$$\Delta(\omega) = \sqrt{\frac{2}{\pi}} \int_{t_0}^{t_s} S(t) \cos \omega(t - t_0) dt \tag{16}$$

The problem is to obtain an approximation for $\Delta(\omega)$ using only $S_1(t)$.

We first obtain an expression for $\Delta(\omega)$ using $\hat{S}(\omega)$:

$$\Delta(\omega) = \sqrt{\frac{2}{\pi}} \int_{t_0}^{t_s} S(t) \cos \omega(t - t_0) dt = \frac{2}{\pi} \int_{t_0}^{t_s} \int_{0}^{\infty} \hat{S}(\omega') \cos \omega'(t - t_0) \cos \omega(t - t_0) d\omega' dt$$

Switching the order of integration to integrate with respect to t first, yields

$$\Delta(\omega) = \frac{1}{\pi} \int_{0}^{\infty} \hat{S}(\omega') \left(\frac{\sin(\omega - \omega')(t_s - t_0)}{\omega - \omega'} + \frac{\sin(\omega + \omega')(t_s - t_0)}{\omega + \omega'} \right) d\omega'$$

Since $\hat{S}(\omega')$ is non-vanishing only around harmonics of the design frequency ω_0, we may neglect the second term in the parentheses to get

$$\Delta(\omega) = \frac{1}{\pi} \int_{0}^{\infty} \hat{S}(\omega') \frac{\sin(\omega - \omega')(t_s - t_0)}{\omega - \omega'} d\omega'$$

as the harmonic frequencies are large in comparison to values of $\sin(\omega - \omega')(t_s - t_0)$.

To extract a suitable approximation of $\Delta(\omega)$, two considerations need to be taken into account. The first is the presence of frequencies outside of the aperture region in $\hat{S}_1(\omega)$. These frequencies do not correspond to actual muon revolution frequencies and so they may be dropped. The second consideration is the fact that the difference between $\hat{S}(\omega)$ and $\hat{S}_1(\omega)$ is very nearly a constant. This can be seen in Figures 9 and 10. Combined, these considerations yield the following approximation for $\Delta(\omega)$ in terms of $\hat{S}_1(\omega)$

$$\Delta(\omega) \approx \frac{1}{\pi} \int_{\omega_1^-}^{\omega_1^+} \hat{S}_1(\omega') \frac{\sin(\omega - \omega')(t_s - t_0)}{\omega - \omega'} d\omega' \tag{17}$$

where (ω_1^-, ω_1^+) is the interval of frequencies corresponding to the location of the first harmonic and muon orbits within the aperture region. Figure 11 features a comparison of the [redacted] $\Delta(\omega)$ (featured in Figure 9) and its approximation.

For more details on this result, see the Appendix.

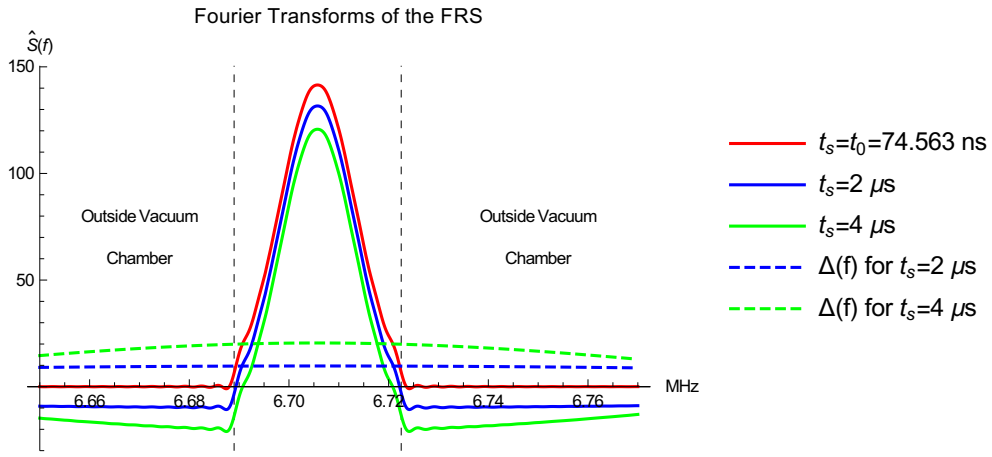

Figure 9: Frequency spectra for the case of a Gaussian energy offset distribution and no longitudinal distribution. Spectra for different t_s are displayed, as well the corresponding $\Delta(f)$ functions. Up to 2000 turns.

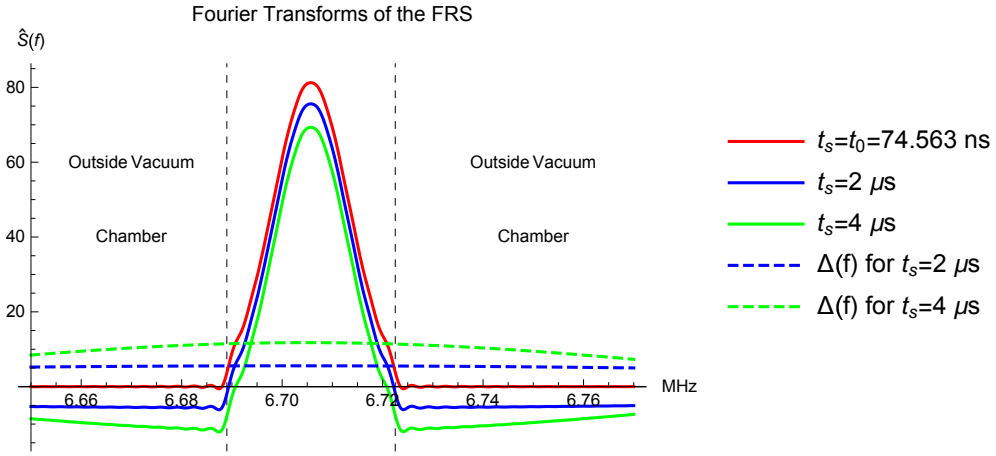

Figure 10: Frequency spectra for the case of a Gaussian energy offset distribution with $\Delta_0 = 0.112\%$ and Gaussian longitudinal spread with $\sigma_t = 25$ ns. Spectra for different t_s are displayed, as well the corresponding $\Delta(f)$ functions. Up to 2000 turns.

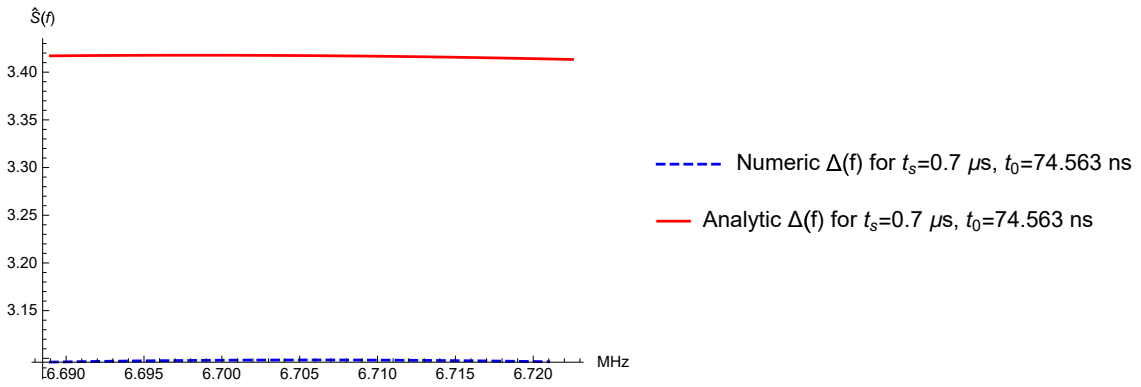

Figure 11: The actual and approximated $\Delta(f)$ functions for the beam of Figure 1 for $t_s = 700\mu$s. The actual and approximated $\Delta(f)$ have spreads of 0.0100987 MHz and 0.0100985 MHz respectively.

In Figure 11 we see a comparison of the approximated (computed numerically) $\Delta(\omega)$ and the actual $\Delta(\omega)$. Their spreads are similar, meaning that the approximation is valid.

3.8 Fourier Analysis Examples

3.8.1 Analysis for a Gaussian Energy Offset Distribution with Initially Zero Bunch Length

The fast rotation signal is given by (6) with momentum offset distribution (7). Suppose the center of mass of the muon beam first passes the detector at time t_0. The frequency spectrum is then

$$\hat{S}(\omega) = \sqrt{\frac{2}{\pi}} \int_{t_0}^{\infty} \sum_{n=0}^{\infty} \frac{\rho\left(\frac{t}{nT+t_0} - 1\right)}{nT + t_0} \cos\omega(t - t_0)dt =$$

$$\sum_{n=0}^{\infty} \frac{\sqrt{2/\pi}}{nT + t_0} \int_{t_0}^{\infty} \rho\left(\frac{t}{nT + t_0} - 1\right) \cos\omega(t - t_0)dt$$

ρ doesn't vanish if its argument in the integral above is contained in $(-\Delta_c, \Delta_c)$, which happens if $(1 - \Delta_c)(nT + t_0) \leq t \leq (1 + \Delta_c)(nT + t_0)$. Therefore the upper bound of the integral is $(1 + \Delta_c)(nT + t_0)$. If $(1 - \Delta_c)(nT + t_0) > t_0$, then the lower bound is given by $(1 - \Delta_c)(nT + t_0)$; otherwise it is given by t_0. Hence the lower bound is given by $\max\{t_0, (1 - \Delta_c)(nT + t_0)\}$.

$$\hat{S}(\omega) = \sum_{n=0}^{\infty} \frac{\sqrt{2/\pi}}{nT + t_0} \int_{\max\{t_0,(1-\Delta_c)(nT+t_0)\}}^{(1+\Delta_c)(nT+t_0)} \frac{\exp\left[-\left(\frac{t}{nT+t_0} - 1\right)^2 / 2\Delta_0^2\right]}{\sqrt{2\pi}\Delta_0} \cos\omega(t - t_0)dt =$$

$$\sum_{n=0}^{\infty} \frac{e^{-\omega^2(nT+t_0)^2\Delta_0^2/2} e^{i\omega nT}}{2\sqrt{2\pi}} \left(\text{Erf}\left[\frac{\Delta_c}{\Delta_0\sqrt{2}} - \frac{i\omega(nT + t_0)\Delta_0}{\sqrt{2}}\right]\right) + c.c.$$

$$-\sum_{n=0}^{\infty} \frac{e^{-\omega^2(nT+t_0)^2\Delta_0^2/2} e^{i\omega nT}}{2\sqrt{2\pi}} \left(\text{Erf}\left[\frac{-1}{\Delta_0\sqrt{2}} - \frac{i\omega(nT + t_0)\Delta_0}{\sqrt{2}} + \max\left[\frac{t_0}{\Delta_0\sqrt{2}(nT + t_0)}, \frac{1 - \Delta_c}{\Delta_0\sqrt{2}}\right]\right]\right) - c.c \tag{18}$$

We now find $\Delta(\omega)$.

$$\Delta(\omega) = \sqrt{\frac{2}{\pi}} \int_{t_0}^{t_s} \sum_{n=0}^{\infty} \frac{\rho\left(\frac{t}{nT+t_0} - 1\right)}{nT + t_0} \cos\omega(t - t_0)dt =$$

$$\sum_{n=0}^{\infty} \frac{\sqrt{2/\pi}}{nT+t_0} \int_{t_0}^{t_s} \rho\left(\frac{t}{nT+t_0}-1\right)\cos\omega(t-t_0)dt =$$

$$\sum_{n=0}^{\infty} \frac{\sqrt{2/\pi}}{nT+t_0} \int_{\max\{t_0,(1-\Delta_c)(nT+t_0)\}}^{\min\{t_s,(1+\Delta_c)(nT+t_0)\}} \frac{\exp\left[-\left(\frac{t}{nT+t_0}-1\right)^2/2\Delta_0^2\right]}{\sqrt{2\pi}\Delta_0}\cos\omega(t-t_0)dt$$

However, we must take into account that (t_0, t_s) and $((1-\Delta_c)(nT+t_0), (1+\Delta_c)(nT+t_0))$ may not intersect at all. This occurs if $n \geq \frac{t_s}{T(1-\Delta_c)} - \frac{t_0}{T}$, so we must sum to $N = \lfloor \frac{t_s}{T(1-\Delta_c)} - \frac{t_0}{T} \rfloor$:

$$\sum_{n=0}^{N} \frac{\sqrt{2/\pi}}{nT+t_0} \int_{\max\{t_0,(1-\Delta_c)(nT+t_0)\}}^{\min\{t_s,(1+\Delta_c)(nT+t_0)\}} \frac{\exp\left[-\left(\frac{t}{nT+t_0}-1\right)^2/(2\Delta_0^2)\right]}{\sqrt{2\pi}\Delta_0}\cos\omega(t-t_0)dt =$$

$$\sum_{n=0}^{N} \frac{e^{-\omega^2(nT+t_0)^2\Delta_0^2/2}e^{i\omega nT}}{2\sqrt{2\pi}}\left(\mathrm{Erf}\left[\frac{-1}{\Delta_0\sqrt{2}} - \frac{i\omega(nT+t_0)\Delta_0}{\sqrt{2}} + \min\left[\frac{1+\Delta_c}{\Delta_0\sqrt{2}}, \frac{t_s}{\Delta_0(nT+t_0)\sqrt{2}}\right]\right]\right) + c.c.$$
$$-\sum_{n=0}^{N} \frac{e^{-\omega^2(nT+t_0)^2\Delta_0^2/2}e^{i\omega nT}}{2\sqrt{2\pi}}\left(\mathrm{Erf}\left[\frac{-1}{\Delta_0\sqrt{2}} - \frac{i\omega(nT+t_0)\Delta_0}{\sqrt{2}} + \max\left[\frac{1-\Delta_c}{\Delta_0\sqrt{2}}, \frac{t_0}{\Delta_0(nT+t_0)\sqrt{2}}\right]\right]\right) - c.c. \tag{19}$$

The Fourier transforms are shown in Figure 9.

3.8.2 Analysis for a Gaussian Energy Offset Distribution and Gaussian Longitudinal Distribution

To make calculations simpler we use a narrow momentum spread, such that a negligible number of muons lie outside the vacuum chamber. We thus have that $\rho(\Delta) = \frac{e^{-\Delta^2/2\Delta_0^2}}{\sqrt{2\pi}\Delta_0}$ and $\xi(t) = \frac{e^{-t^2/2\sigma_t^2}}{\sqrt{2\pi}\sigma_t}$. For clarity, we write $nT + t_0$ as nT.

$$\begin{aligned}
S(t) &= \sum_{n=0}^{\infty}\int_{-\infty}^{\infty} dt' \frac{e^{-\left(\frac{t-t'}{nT}-1\right)^2/2\Delta_0^2}}{\sqrt{2\pi}\Delta_0 nT}\frac{1}{\sqrt{2\pi}\sigma_t}e^{-t'^2/2\sigma_t^2} \\
&= \sum_{n=0}^{\infty}\frac{1}{2\pi\Delta_0 nT\sigma_t}\int_{-\infty}^{\infty} dt' e^{-\left(\frac{t-t'}{nT}-1\right)^2/2\Delta_0^2}e^{-t'^2/2\sigma_t^2} \\
&= \sum_{n=0}^{\infty}\frac{1}{2\pi\Delta_0 nT\sigma_t}e^{-t^2/(2(nT\Delta_0)^2)}\int_{-\infty}^{\infty} dt' e^{-\left(\frac{t'^2-2tt'}{(nT)^2}+1-\frac{2(t-t')}{nT}\right)/2\Delta_0^2}e^{-t'^2/2\sigma_t^2} \\
&= \sum_{n=0}^{\infty}\frac{1}{2\pi\Delta_0 nT\sigma_t}e^{-t^2/(2(nT\Delta_0)^2)}e^{\frac{t}{nT\Delta_0^2}}\int_{-\infty}^{\infty} dt' \exp\left(-t'^2\left(\frac{1}{2(nT)^2\Delta_0^2}+\frac{1}{2\sigma_t^2}\right)+t'(\frac{t}{nT}-1)/(nT\Delta_0^2)\right)e^{-1/2\Delta_0^2} \\
&= \sum_{n=0}^{\infty}\frac{1}{2\pi\Delta_0 nT\sigma_t}e^{-\left(\frac{t}{nT}-1\right)^2/2\Delta_0^2}\int_{-\infty}^{\infty} dt' \exp\left(-\alpha t'^2+\beta t'\right) \\
&= \sum_{n=0}^{\infty}\frac{1}{2\pi\Delta_0 nT\sigma_t}e^{-\left(\frac{t}{nT}-1\right)^2/2\Delta_0^2}\sqrt{\frac{\pi}{\alpha}}e^{\beta^2/4\alpha}
\end{aligned}$$

where $\alpha = \frac{1}{2(nT)^2\Delta_0^2} + \frac{1}{2\sigma_t^2}$ and $\beta = (\frac{t}{nT} - 1)/(nT\Delta_0^2)$. Finally

$$\begin{aligned} S(t) &= \sum_{n=0}^{\infty} \frac{1}{2\pi\Delta_0 nT\sigma_t} e^{-\left(\frac{t}{nT}-1\right)^2/2\Delta_0^2} \frac{\sqrt{2\pi}nT\Delta_0\sigma_t}{\sqrt{(nT)^2\Delta_0^2+\sigma_t^2}} \exp\left(\frac{\left(\frac{t}{nT}-1\right)^2}{(nT\Delta_0^2)^2} \frac{(nT)^2\Delta_0^2\sigma_t^2}{2(nT)^2\Delta_0^2+2\sigma_t^2}\right) \\ &= \frac{1}{\sqrt{2\pi}} \sum_{n=0}^{\infty} e^{-\left(\frac{t}{nT}-1\right)^2/2\Delta_0^2} \frac{1}{\sqrt{((nT)^2\Delta_0^2+\sigma_t^2}} \exp\left(\frac{\left(\frac{t}{nT}-1\right)^2}{\Delta_0^2} \frac{\sigma_t^2}{2(nT)^2\Delta_0^2+2\sigma_t^2}\right) \\ &= \frac{1}{\sqrt{2\pi}} \sum_{n=0}^{\infty} \frac{1}{\sqrt{((nT)^2\Delta_0^2+\sigma_t^2}} \exp\left(\frac{-\left(\frac{t}{nT}-1\right)^2}{2\Delta_0^2}\left(1 - \frac{\sigma_t^2}{(nT)^2\Delta_0^2+\sigma_t^2}\right)\right) \end{aligned} \tag{20}$$

It will turn out to be convenient to rewrite Equation 20 as

$$S(t) = \frac{1}{\sqrt{2\pi}} \sum_{n=0}^{\infty} \frac{1}{(nT)\Delta_0'} \exp\left(\frac{-(\frac{t}{nT}-1)^2}{2{\Delta_0'}^2}\right) \tag{21}$$

where

$${\Delta_0'}^2 = \frac{(nT\Delta_0)^2+\sigma_t^2}{(nT)^2}$$

Proceeding with the Fourier transform,

$$\hat{S}(\omega) = \sqrt{\frac{2}{\pi}} \int_{t_0}^{\infty} S(t)\cos\omega(t-t_0)dt = \int_{t_0}^{\infty} S(t)\frac{e^{i\omega(t-t_0)}+e^{-i\omega(t-t_0)}}{2}dt$$

From a table of integrals, we have that

$$\int_u^{\infty} \exp\left(-\frac{x^2}{4\beta} - \gamma x\right)dx = \sqrt{\pi\beta}e^{\beta\gamma^2}\left(1 - \frac{\sqrt{\pi}}{2}\mathrm{Erf}\left[\gamma\sqrt{\beta} + \frac{u}{2\sqrt{\beta}}\right]\right)$$

Applying this formula yields

$$\hat{S}(\omega) = \frac{1}{\sqrt{2\pi}} \sum_{n=0}^{\infty} e^{-(\omega(nT)\Delta_0')^2/2)}\left(e^{i\omega(nT)}\left(1 - \frac{\sqrt{\pi}}{2}\mathrm{Erf}\left[\frac{-1}{\Delta_0'\sqrt{2}} - \frac{i\omega(nT)}{\sqrt{2}} + \frac{t_0}{\Delta_0'(nT)\sqrt{2}}\right]\right) + c.c.\right)$$

$$\begin{aligned} \Delta(\omega) = &\\ &\frac{1}{\sqrt{2\pi}} \sum_{n=0}^{\infty} e^{-(\omega(nT)\Delta_0')^2/2)}\left(e^{i\omega(nT)}\left(1 - \frac{\sqrt{\pi}}{2}\mathrm{Erf}\left[\frac{-1}{\Delta_0'\sqrt{2}} - \frac{i\omega(nT)}{\sqrt{2}} + \frac{t_0}{\Delta_0'(nT)\sqrt{2}}\right]\right) + c.c.\right) \\ &-\frac{1}{\sqrt{2\pi}} \sum_{n=0}^{\infty} e^{-(\omega(nT)\Delta_0')^2/2)}\left(e^{i\omega(nT)}\left(1 - \frac{\sqrt{\pi}}{2}\mathrm{Erf}\left[\frac{-1}{\Delta_0'\sqrt{2}} - \frac{i\omega(nT)}{\sqrt{2}} + \frac{t_s}{\Delta_0'(nT)\sqrt{2}}\right]\right) + c.c.\right) \end{aligned} \tag{22}$$

We see the Fourier transforms in Figure 10.

4 Appendix

4.1 Corrections to the Fourier Transform

Here we expand on the derivation of the approximation for $\Delta(\omega)$ in Equation (17). We discuss in detail how two considerations result in the approximation.

4.1.1 First Consideration

The FRS arises due to the periodic detector hits of the muons, with each muon orbiting within the aperture of the vacuum chamber thus defining the allowed frequencies and their harmonics. If we instead Fourier analyze $S_1(t)$, then the fact that it is identically zero on (t_0, t_s) necessarily gives rise to frequencies in $\hat{S}_1(\omega)$ that lie outside the harmonics. These new frequencies obviously do not correspond to muons and are merely an indication of our ignorance of the beam's behavior on (t_0, t_s).

4.1.2 Second Consideration

Consider the Heisenberg uncertainty principle for Fourier transforms. It states that given a function $f(t)$ with mean $f(\bar{t})$ and its Fourier transform $\hat{f}(\omega)$ with mean $\hat{f}(\bar{\omega})$, their standard deviations satisfy the inequality

$$\sigma(f(t))\sigma(\hat{f}(\omega)) = \left(\int_{-\infty}^{\infty}(t-\bar{t})^2|f(t)|^2dt\right)^{1/2}\left(\int_{-\infty}^{\infty}(\omega-\bar{\omega})^2|\hat{f}(\omega)|^2d\omega\right)^{1/2} \geq \frac{1}{4\pi}$$

The contribution to $\sigma(\hat{S}(\omega))$ comes from the harmonics of $\hat{S}(\omega)$, since everywhere else the Fourier transform vanishes. In other words

$$\sigma(\hat{S}(\omega)) = \left(\sum_{n=1}^{\infty}\int_{\omega_n^-}^{\omega_n^+}\omega^2|\hat{S}(\omega)|^2d\omega\right)^{1/2}$$

where the n-th harmonic lies in (ω_n^-,ω_n^+). $\hat{S}_1(\omega)$ and $\Delta(\omega)$ also have harmonics but additionally feature frequencies outside them. By the discussion of the previous section, we may disregard these external frequencies. If the interval (t_0,t_s) is small, we then expect that $\sigma(\Delta(\omega)) > \sigma(\hat{S}_1(\omega)) \approx \sigma(\hat{S}(\omega))$ since $S_1(t)$ and $S(t)$ are observed on larger time windows. Since the contributions for each of $\sigma(\Delta(\omega))$, $\sigma(\hat{S}_1(\omega))$,$\sigma(\hat{S}(\omega))$ come from their individual harmonics, we must have that

$$\sigma_n(\Delta(\omega)) = \left(\int_{\omega_n^-}^{\omega_n^+}\omega^2|\Delta(\omega)|^2d\omega\right)^{1/2} > \left(\int_{\omega_n^-}^{\omega_n^+}\omega^2|\hat{S}_1(\omega)|^2d\omega\right)^{1/2} \approx \left(\int_{\omega_n^-}^{\omega_n^+}\omega^2|\hat{S}(\omega)|^2d\omega\right)^{1/2} = \sigma_n(\hat{S}(\omega))$$

for each harmonic. We thus expect $\Delta(\omega)$ to appear nearly constant on all intervals (ω_n^-,ω_n^+) due to its large standard deviation there.

Recalling that $\hat{S}(\omega) = \hat{S}_1(\omega) + \Delta(\omega)$, and observing that $\hat{S}(\omega) \approx \hat{S}_1(\omega) + \text{const.}$ in the vicinity of a harmonic, we thus see that

$$\frac{1}{\pi}\int_{\omega_1^-}^{\omega_1^+}\hat{S}_1(\omega')\frac{\sin(\omega-\omega')(t_s-t_0)}{\omega-\omega'}d\omega' = \frac{1}{\pi}\int_{\omega_1^-}^{\omega_1^+}\hat{S}(\omega')\frac{\sin(\omega-\omega')(t_s-t_0)}{\omega-\omega'}d\omega' - \frac{\text{const.}}{\pi}\int_{\omega_1^-}^{\omega_1^+}\frac{\sin(\omega-\omega')(t_s-t_0)}{\omega-\omega'}d\omega' =$$

$$\Delta(\omega) - \frac{\text{const.}}{\pi}\int_{\omega_1^-}^{\omega_1^+}\frac{\sin(\omega-\omega')(t_s-t_0)}{\omega-\omega'}d\omega'$$

In the vicinity of the magic frequency f_0 the integrand in the line above may be Taylor expanded (since $(t_s-t_0)(f-f_0)$ is small) and the whole expression becomes

$$\Delta(\omega) - \frac{\text{const.}(t_s-t_0)}{\pi}\int_{\omega_1^-}^{\omega_1^+}\left(1-\frac{(\omega-\omega')^2(t_s-t_0)^2}{6}\right)d\omega' =$$

$$\Delta(\omega) - O(1)$$

Therefore

$$\Delta(\omega) = \frac{1}{\pi}\int_{\omega_1^-}^{\omega_1^+}\hat{S}_1(\omega')\frac{\sin(\omega-\omega')(t_s-t_0)}{\omega-\omega'}d\omega' + O(1)$$

References

[1] Yuri Orlov, Cenap S. Ozben, and Yannis K. Semertzidis. Muon revolution frequency distribution from a partial-time fourier transform of the g-2 signal in the muon g-2 experiment. *Nucl. Instrum. Methods Phys. Res. A*, 482:9, 2002.